Peroxide Assisted Coupling and Characterization of Carbon-Nanofiber-Reinforced Poly(propylene) Composites

A. de la Vega Oyervides, J. Bonilla Ríos,* L. F. Ramos de Valle, L. A. S. de Almeida Prado, Karl Schulte

The purpose of this work is the enhancement of the interfacial interactions between isotactic poly(propylene) and carbon nanofibers. A free radical coupling reaction was carried out by heat assisted peroxide oxidation of the nanofibers prior to their incorporation to an isotactic poly(propylene) matrix. The materials were characterized through SEM, DSC, DMTA and tensile testing. An increase of up to 17% in the Young's modulus of treated to untreated composites was attained. In combination with DSC analysis, the tensile data did not point to a possible correlation between increased stiffness and increased crystallinity. The mechanical performance of the modified composites is believed to be due to two combined opposite effects: increased chemical interaction at the interface, and peroxide-induced isotactic poly(propylene) degradation.

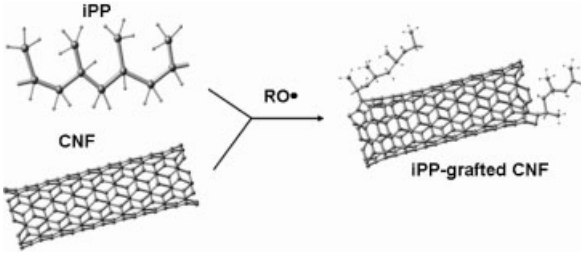

Introduction

In recent years, carbon nanotubes and carbon nanofibers have widely been investigated as fillers for polymeric composites due to their outstanding mechanical, thermal and electrical properties.[1–3] These features, combined with their very high surface area to volume ratio, make them very promising candidates for the development of ultra low-weight engineering and multifunctional polymeric materials.[3–9] Carbon nanofibers (CNFs), produced by the catalytic decomposition of hydrocarbons at the vapor-phase, have diameters ranging from 5 to 200 nm and lengths up to 100 μm.[4,10,11] Their high aspect ratio and graphitization degree make them an attractive choice for the manufacturing of advanced polymeric materials with improved strength and stiffness, as well as some supplementary attributes such as electrical conductivity and improved thermal stability.[4,5,9,11] Moreover, vapor grown carbon nanofibers suppose a relatively low cost

A. de la Vega. Oyervides, J. Bonilla Ríos
Centro de Innovación en Diseño y Tecnología, Instituto Tecnológico y de Estudios Superiores de Monterrey, 64849 Monterrey, México
Fax: +52 (81) 83-28-41-23; E-mail: jbonilla@itesm.mx
L. F. Ramos de Valle
Centro de Investigación en Química Aplicada (CIQA), 25253 Saltillo, México
A. de la Vega, Oyervides, L. A. S. de Almeida Prado, K. Schulte
Institute of Polymers and Composites, Technische Universität Hamburg-Harburg, 21073 Hamburg, Germany

DOI: 10.1002/mame.200700201

model system for carbon nanotubes in order to understand their role for load transfer in composites.[12]

Vapor grown carbon fibers (VGCFs) have been successfully compounded with different thermoplastic[9,10,12–25] and thermoset[26,27] matrices using conventional polymer processing technology such as high-shear mixing or extrusion, demonstrating the feasibility of such methods for effective dispersion and orientation of the nanofibers. Unfortunately, the mechanical performance of these composites have been limited by the lack of an adequate interface strength, which results in poor interlaminar adherence and fiber pull-out.[4,28]

Studies presented by Lozano et al.[9,23] upon the properties of nanofiber-reinforced thermoplastic composites, using purified VGCF in a poly(propylene) matrix, demonstrated that the stiffness of the composites could be enhanced by several orders of magnitude compared to that of neat poly(propylene). However, the negligible effect upon the tensile strength was attributed to a brittleness of the material due to changes in crystallinity.

More recently, Brandl et al.[24] attempted the production of VGCF/poly(propylene) composites with fibers functionalized via cold plasma. Water contact angle measurements confirmed the enhancement of the hydrophilicity of the fibers, hence enabling effective wetting by the matrix without detriment of their structure. An increase of 16% in tensile strength, and 18% in Young's Modulus of the functionalized fiber-composites could be attained.

Other attempts to overcome the CNF-poly(propylene) incompatibility and achieve a stronger interface include those of Kelarakis, Hsiao and Chu,[14,15] in which a suspension-procedure was used to graft short poly(propylene) chains onto the surface of the nanofibers with the use of maleic anhydride grafted poly(propylene), in order to avoid nanofiber aggregation and enhance compatibility with polyolefins and elastomers.

Finegan and Tibbetts,[20] used a variety of wet-chemistry and oxidation methods, including air-etching and CO_2 oxidization, to impart some acidic functionality to as-grown carbon nanofibers synthesized at different conditions. Tensile testing demonstrated that both the modulus and yield stress of the neat poly(propylene) could be tripled at 15% content of CO_2 oxidized and air-etched nanofibers, as a result of an increased surface area and energy.

The difficulty in attaining a good interfacial adhesion in a CNF-poly(propylene) system is owed to the low surface energy of poly(propylene)[29] and high hydrophobicity of the nanofibers in the pristine state due to their graphitic perfection. In the present work, we intended the use of organic peroxides as free-radical generators at the terminal double bonds of the fiber, for enhanced interaction with isotactic poly(propylene) (iPP) macro-radicals generated during shear or peroxide-assisted degradation.

Experimental Part

Materials

Pyrograf III vapor grown-carbon fibers (PR-24-AG) were supplied by Applied Science Inc. These CNFs are 100 to 200 nm in diameter and up to 100 μm long, with a density of 1.95 $g \cdot cm^{-3}$ and a surface area of approximately 20 $m^2 \cdot g^{-1}$. The fibers were functionalized with a solution of a 2,5-dimethyl-2,5-di(*t*-butylperoxy) hexane peroxide (Luperox 101; here coded as L-101, by Arkema Inc.) diluted in acetone, and preheated to the activation temperature of the initiator (≈190 °C).

An isotactic poly(propylene) homopolymer (iPP Stamylan iPP 578 P, by Sabic Europe) with a melt flow index of 25 $g \cdot 10\ min^{-1}$ at 230 °C and density of 0.905 $g \cdot cm^{-3}$ was selected as the polymeric matrix.

Preparation and Processing

The peroxide solution was prepared by diluting 1, 3 and 5 ppm of Luperox 101 (ppm with respect to the PP/CNF mixture weight) in a sufficient amount of acetone to attain a 1:1 relation of fiber to the Luperox solution by weight. Such a relation helped to ensure a complete impregnation of the CNFs. The wetted fibers were then heated in a vacuum oven, first at 60 °C for 1 h to evaporate the acetone, and subsequently, at 190 °C for 30 min to activate the peroxide. Before compounding, the poly(propylene) was pulverized in a laboratory ball mill, for which, the iPP pellets were previously introduced in liquid nitrogen for 10 min.

All composites were produced with a constant fiber content of 1 wt.-%. A lab-twin screw extruder from Haake (Rheomex PTW16/25) was used to prepare the composites. Operation conditions are shown in Table 1. The fibers were manually pre-mixed with the pulverized iPP and the mixture was dosed into the extruder. The composite strands were then re-pelletized and injection-molded by means of a hydraulic microinjector Babyplast 6/10 machine operated at 200 °C, to obtain tensile specimens according to ASTM D-680. The specimens were 80 mm long and 5 mm wide in the testing zone, with an average thickness of 2 mm. These specimens were used for both the tensile and the dynamical-mechanical characterization.

Composite Characterization

The different samples were identified as iPP (unfilled isotactic poly(propylene)); NC_POx:00 (with untreated or reference CNFs);

Table 1. Operating conditions of the twin screw extruder.

Parameter	Value
Temp. at heating zone 1	190 °C
Temp. at heating zone 2	195 °C
Temp. at heating zone 3	205 °C
Temp. at die	210 °C
Screws rotation speed	55 rpm

Macromol. Mater. Eng. **2007**, *292*, 1095–1102

Macromolecular Journals
DOI: 10.1002/mame.200700201

and NC_POx:01, NC_POx:03 and NC_POx:05 for the composites with 1, 3 and 5 ppm peroxide treated CNFs, respectively.

The effect of the oxidative treatment on the structure of the nanofibers was monitored through Raman spectroscopy. The spectra were recorded at room temperature by means of a Jobin Yvon LabRaman HR 800 spectrometer, with a 633 nm laser, and a power output of 20 mW.

A gel permeation chromatograph V-2000, with a refraction index detector and "styragel" columns, was used to determine the molecular weight distribution of the neat and reinforced iPP. The samples were first dissolved in tri-chlorobenzene and run in the GPC at 140 °C, at a flow rate of 1 mL · min^{-1}.

Information concerning the crystallinity of the samples was obtained with a Seiko DSC SSC 5200 differential scanning calorimeter. The measurements were made under a nitrogen atmosphere from −50 to 220 °C, at a heating rate of 10 °C · min^{-1}.

Dynamical mechanical thermal analysis (DMTA) was performed in an Eplexor 500 N instrument by Gabo Qualimeter, operated in tensile mode. The temperature range analyzed was −50 to 150 °C, at a constant frequency of 1 Hz.

Tensile tests were performed in a United SFM instrument, according to ASTM-638. The deformation rate was 12.7 mm · min^{-1}, and a minimum of 5 tests were made for each sample. The Young's modulus was calculated from the slope of the stress-strain curve up to the elastic limit.

Scanning electron microscopy (SEM) images were obtained by means of a L1530 scanning electronic microscope, from Leo Instruments. For their observation, the composites were fractured at liquid nitrogen temperature, and the exposed surfaces were analyzed without sputtering.

Results and Discussion

The two naturally occurring peaks in the Raman spectra of carbon structures, namely the D and G band, are found in carbon nanofibers at around 1360 and 1580 cm^{-1}, respectively.[30] These features provide information about the structural integrity of the material. The ratio of the D to G peak intensities (I_D/I_G) can be used as an indicator of the amount of carbon defect sites due to the presence of functional groups (disordered structure or amorphous carbon) relative to the graphitic planes. In Figure 1, the Raman spectra of the untreated and treated CNFs have been normalized to the intensity of the G peak, and superposed. It can be seen that the peroxide treatment with a concentration of 0.01 wt.-% (equivalent to 1 ppm) did not vary significantly from the D-band intensity of the untreated CNFs; whereas at higher peroxide concentration (i.e., 0.05 wt.-%), the intensity of the D-band increases by a factor of 1.16, indicating a greater amount of carbon defects due to the presence of functional groups, promoted by the peroxide treatment. These groups in the graphitic planes of the CNFs stand for potentially active sites for the occurrence of interactions between the CNFs and the polymer chains, increasing the compatibility and facilitating the mixing process.

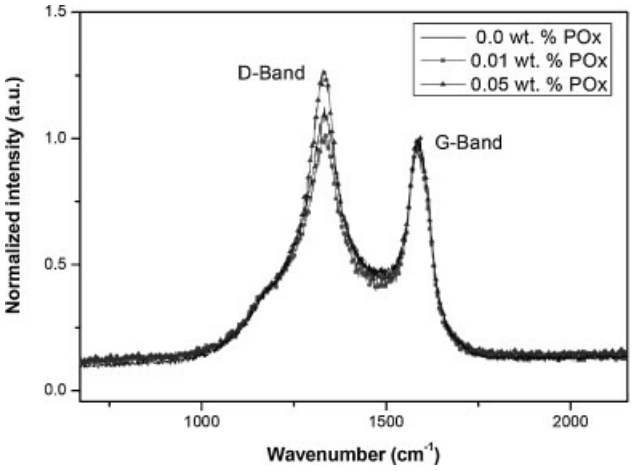

Figure 1. D and G bands in the Raman spectra of three types of nanofibers.

Physical transitions as well as crystalline fraction of the neat and CNF-filled poly(propylene) were determined from the non-isothermal DSC measurements. The heating curves (Figure 2) revealed that the melting temperature T_m remained unchanged after the addition of the fibers, whether the untreated or the peroxide treated CNFs were utilized. However, an evident increase in the melting peak area is observed, suggesting an increase in the crystalline fraction X_c of the sample.

For any given sample, the crystalline fraction X_c can be determined from the melting curve data as:[31]

$$X_c = \frac{\Delta H_f}{\Delta H_f^{\circ} \times F} \quad (1)$$

Where ΔH_f is given by the area under the endotherm, and ΔH_f° is the theoretical melting enthalpy for a 100%

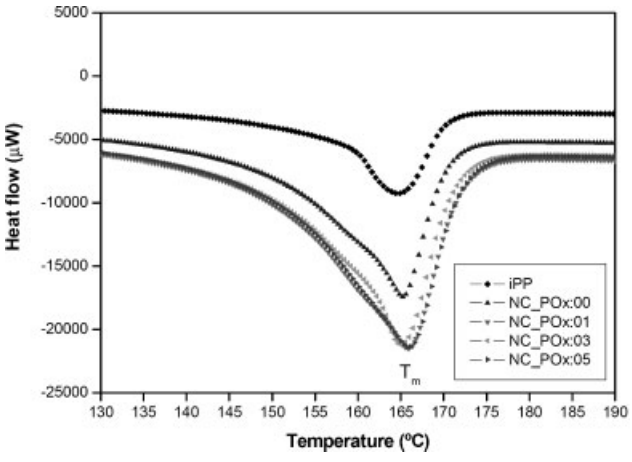

Figure 2. DSC curve for iPP and iPP/CNF during the second heating.

crystalline isotactic poly(propylene), reported as 207 $J \cdot g^{-1}$ by Ehrenstein.[31] The factor F was introduced to account for the actual percentage of poly(propylene) contained in the samples. In this case, all the composites were prepared with 1% of nanofiber, and therefore $F = 0.99$. The values obtained from this analysis are summarized in Table 2.

From the cooling cycle, presented in Figure 3, the effect on the crystallization temperature T_c is evident. The crystallization peak for the composites is shifted from that of the unfilled poly(propylene) by as much as +12 °C. This change in T_c is attributed to the role of the CNFs as nucleating agents for the crystallization of iPP; in particular, for the sample containing 1 ppm of L-101 (NC_Pox:01) the highest shift of the peak is observed. The fact that this effect does not become more pronounced at further peroxide concentrations can be attributed to the degrading effect onto the poly(propylene), resulting in the shortening of the chain lengths. In fact, the GPC measurements confirmed a reduction in the average molecular weight of the composite samples submitted to the peroxide treatment from that of the reference composite (NC_Pox:00). The $\overline{M}_n$ value drops from 150 000 to 132 000 and the polydispersity index $\overline{M}_w/\overline{M}_n$ from 4.16 to 3.74, from the reference composite to that with the highest content of peroxide.

The nucleating effect attributed to the nanofibers is also reflected by an increase in the crystallinity of the composites of up to 14% from that of neat poly(propylene). However, while T_c remains unchanged regardless the fiber treatment, it is seen that the crystalline fraction is affected by peroxide contents above 1 ppm, leading to a decrease of this property, which is associated to the poly(propylene) degradation.

In addition, the melting peak becomes much broader for the nanoreinforced composites in comparison to the neat iPP sample. This fact may be explained in terms of a broader distribution of the thickness of the crystalline lamellae of the polymer due to the presence of the CNFs.[31]

The viscoelastic behavior of the composites was characterized via dynamic mechanical thermal analysis (DMTA). From Figure 4, the reinforcing effect of the fibers is easily observed, especially above the glass transition

Table 2. Non-isothermal DSC results for the measured samples.

Sample	T_c	T_m	X_c
	°C	°C	%
iPP	118.0	165.0	43.4
NC_POx:00	129.7	166.5	57.5
NC_POx:01	131.1	166.6	58.0
NC_POx:03	130.0	166.6	49.6
NC_POx:05	130.0	166.0	43.4

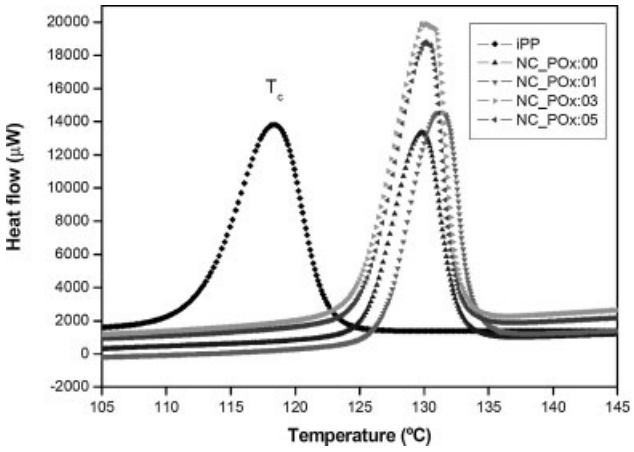

Figure 3. DSC curve for iPP and iPP/CNF composites during the second cooling.

temperature (≈10 °C). The storage modulus of the composites is increased by around 8% at −20 °C, 16% at 20 °C and up to 27% at 50 °C, in comparison to neat iPP. Additionally, no appreciable change in stiffness seems to be related to the different treatments performed onto the fiber above room temperature, since the storage modulus remains unchanged for the different composites at this temperature range. Below the glass transition, the elastic (storage) modulus of poly(propylene) and its composites is related to the segmental γ-motion of the polymer chains, which is, in turn, expectedly hindered by the addition of the nanofibers. It is seen, for the composites with the peroxide treated nanofibers, that those with the lowest CNF content present a seemingly more elastic behavior at this region, resembling that of the reference composite material (NC_POx:00). This is consistent with the observations drawn from the DSC data, since it is expected that a more crystalline material would show higher stiffness.

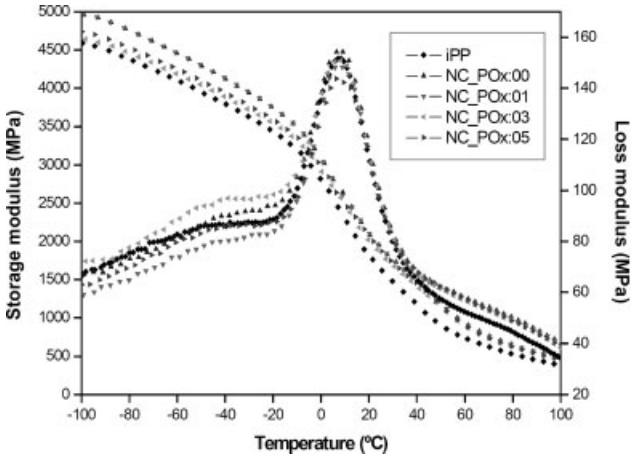

Figure 4. DMTA traces (storage and loss modulus) for the different samples.

Macromol. Mater. Eng. **2007**, *292*, 1095–1102

DOI: 10.1002/mame.200700201

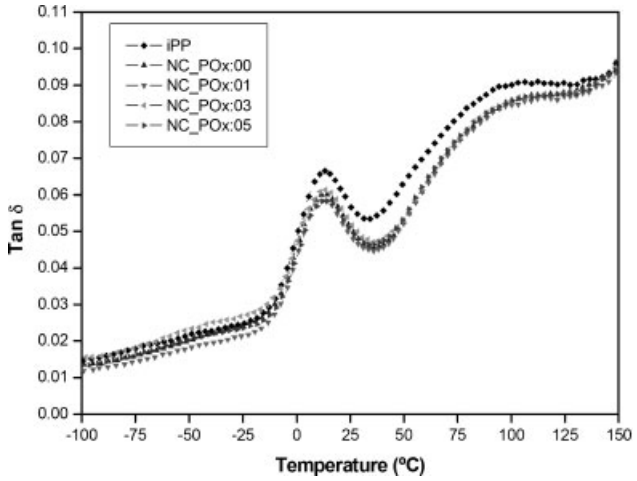

Figure 5. DMTA traces (loss factor or tan δ) for the different samples.

The loss factor (tan δ) plot, presented in Figure 5, shows that the variation in the nanofiber concentration is not associated to a change of the glass transition temperature T_g, since it remains within the same value for the different samples. The T_g gives an indication of a material's transition from ductile to brittle, due to the restrained mobility of the polymeric chains. It can be inferred that at such low nanofiber content, no significant changes on the molecular dynamics of the poly(propylene) were produced.

Figure 6 and Table 3 show the ultimate tensile strength and percent elongation results for the different samples. With the addition of the fibers, the stress-strain response of the material resembles more that of a pure elastic material, in contrast to the typical behavior displayed by poly(propylene), resulting in a dramatic reduction of elongation at break from around 250 to around 30%. This effect can be expected, firstly due to the addition of filler

Table 3. Tensile properties of the measured samples (standard deviations in brackets).

Sample	Tensile Strength	Tensile Modulus	Elongation
	MPa	MPa	%
iPP	35.9 (3.54)	1 344 (101.3)	251 (4.15)
NC_POx:00	36.3 (1.73)	13 205 (132.6)	34.9 (9.58)
NC_POx:01	36.6 (2.46)	1 200 (159.8)	36.3 (7.23)
NC_POx:03	38.3 (1.3)	1 536 (124.8)	30.4 (8.38)
NC_POx:05	36.3 (1.22)	1 314 (240.2)	22.9 (7.41)

and, secondly, due to the increased crystallinity content in the composites. The tensile elongation is not influenced by the peroxide treatment of the nanofibers, indicating that the fiber load plays a significant role in the deformability of the composite. The influence of the peroxide upon the tensile strength of the composites is not as easily observed. The average values for the samples of this series are found within experimental scattering, with the exception of sample NC_Pox:03, which displayed an increment of around 5.5% on tensile strength with respect to unreinforced poly(propylene). At a further concentration level of peroxide, the tensile strength was again decreased, as expected from the observations drawn from DMTA and DSC analysis.

In Figure 7, the average Young's modulus values for the composite series are presented. An increase of 16.5% was found for the NC_Pox:03 sample, when compared to the reference composite NC_Pox:00. The changes in Young's modulus reflect more or less the tendency found for the tensile strength data. It is noticed that at the lowest peroxide content no enhancement is promoted, since the

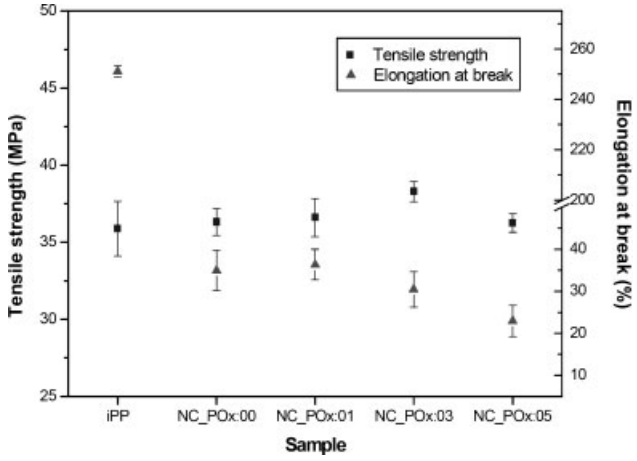

Figure 6. Tensile properties of the iPP/CNF composites.

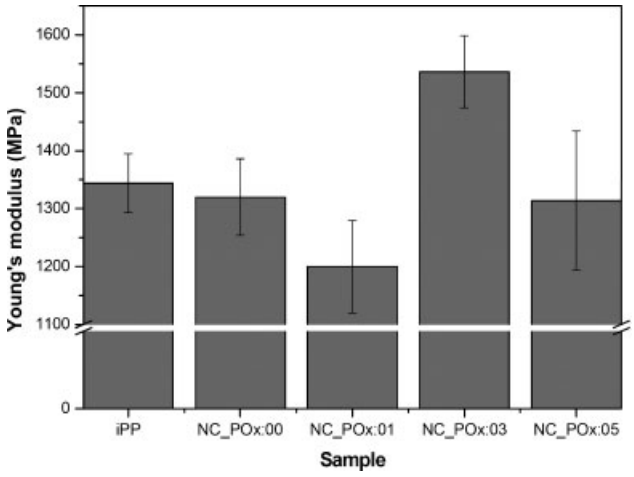

Figure 7. Tensile Modulus of the iPP/CNF composites.

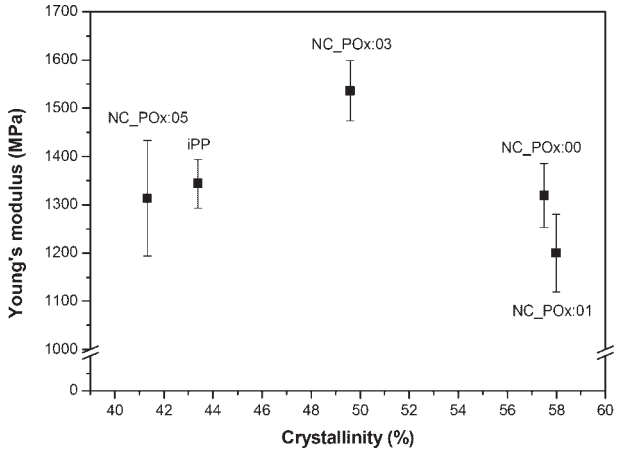

Figure 8. Young's modulus as a function of percent crystallinity for the CNF-iPP composites.

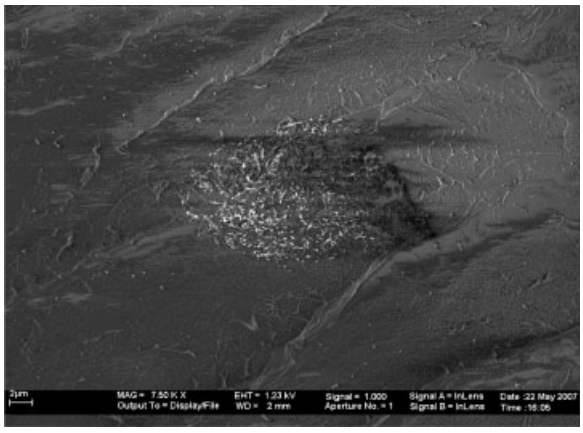

Figure 9. SEM image of the NC_POx:01 sample (10 000X).

amount of initiator is too low to cause any effect on the composite's properties. As the peroxide concentration increases, the modulus reaches a maximum and then begins to drop again because of a more extensive degradation of the iPP chains.

In Figure 8, the Young's modulus is plotted as a function of the degree of crystallinity. There seems to be no direct relation between the modulus and the degree of crystallinity, from which it seems likely that several processes take place during the interaction of the peroxide and the composite's constituents. The authors believe that energy requirements as well as availability of sites for reaction favor in the first place the oxidation of the CNF, followed by the opening of its terminal double bonds and, finally, the degradation of the poly(propylene). The coexistence of CNF and iPP radicals would possibly lead to a covalent bonding at the fiber-matrix interface, at the same time that the CNF bundles can act as nucleation sites for iPP crystallization. It is believed that the two stronger effects in determining the Young's modulus of the composites are the interfacial strengthening and the iPP degradation. Therefore, an optimal point is reached (NC_POx:03) at which the first effect is compensating the latter by the maximum difference. In comparison to the reference composite NC_POx:00, the sample containing 1 ppm of peroxide (NC_POx:01) presented a slightly lower Young's modulus, at about the same crystalline fraction. It is possible that at such conditions, CNFs undergo preferably an oxidation reaction, yielding in the formation of polar groups which further hinder the miscibility with poly(propylene). At 3 ppm peroxide, the crystalline fraction decreases and the modulus increases, given that more iPP chains start to be shortened during the generation of free radicals. Finally, at 5 ppm peroxide, the number of shortened chains exceeds greatly the amount of CNF-iPP bonds created, and so both the modulus and the crystallinity are decreased.

Figure 9 and 10 depict an approximation to a fiber-bunch zone of sample NC_POx:00 in the SEM analysis. A good dispersion of the fibers was observed, although a few agglomerates around 10 μm in diameter, surrounded by large polymer-rich domains, were encountered. Despite being scarcely found throughout the sample, the size of said agglomerates indicates that the fiber dispersion via the extrusion process is not yet optimal. In a closer approximation to the bundle (Figure 10), the occurrence of several fiber-pullouts was observed, suggesting the lack of a strong iPP-CNF interface. Within the agglomerate, the fibers appear close to each other but without forming bundles, indicating a good wettability by the polymer.

Significant improvement of the fiber wettability by the polymer could be regarded as being due to the peroxide treatment, as illustrated by the SEM micrographs of sample NC_POx:03 (Figure 11 and 12). The polymer wrapping around the fibers can be noticed, both in the

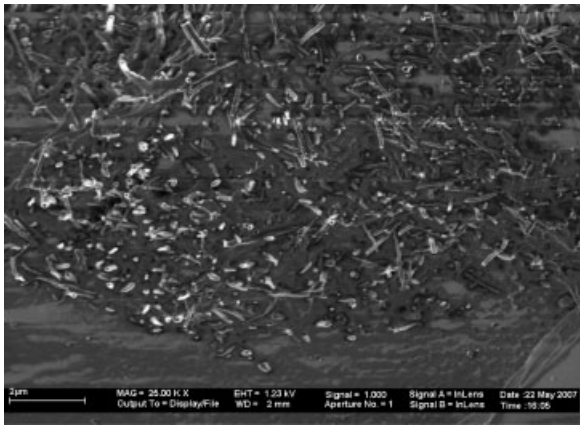

Figure 10. SEM image of the NC_POx:01 sample (30 000X).

Macromol. Mater. Eng. **2007**, *292*, 1095–1102

DOI: 10.1002/mame.200700201

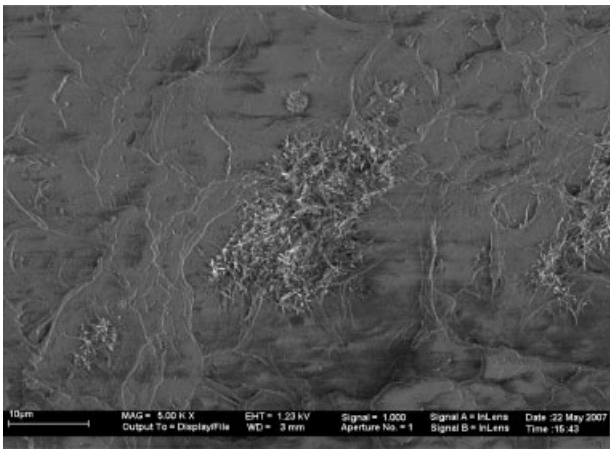

Figure 11. SEM image of the NC_POx:03 sample (10 000X).

outer shell and inner core of the agglomerate (Figure12). The occurrence of some bundles of entangled fibers, in which the polymer was not fully able to penetrate, can also be seen, although both bundles and individual fibers appear to be well embedded. Very occasional pullouts were observed, for which is believed that the peroxide treatment aid in the strengthening of the interface. On the other hand, similar characteristics to the reference composite (NC_POx:00) regarding size and occurrence of fiber agglomerates were found for this sample, indicating a negligible effect of the peroxide on the fiber dispersion.

The dispersion state of the filler has a strong correlation to the mechanical properties of the composites. In this work similar dispersion characteristics between the two kinds of composites (with treated and untreated fibers) were observed, and only the interface was found to be improved by the addition of the peroxide. Said interface improvement played an important role upon the strengthening of the material.

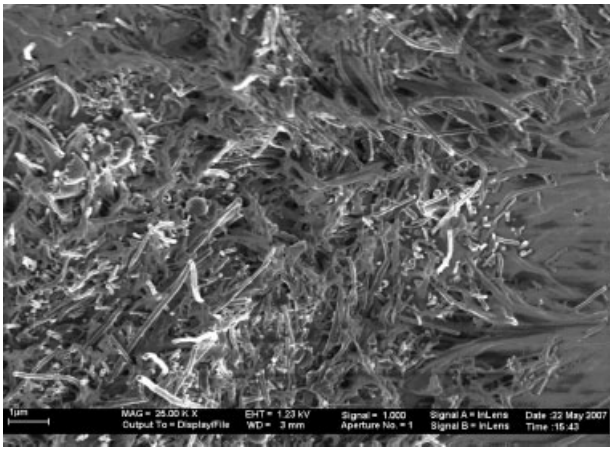

Figure 12. SEM image of the NC_POx:03 sample (30 000X).

Conclusion

The feasibility of the use of organic peroxides as free-radical coupling promoters in a CNF-iPP composite was evidenced by the changes in microstructure and elastic behavior. The tensile properties of the composite were favored by intermediate concentrations of the peroxide initiator, suggesting the occurrence of a bonding reaction at the interface, and therefore a more effective stress transfer mechanism. An increment of around 17% in Young's modulus was attained by pre-treating the fibers with only 3 ppm of L-101, in comparison to the reference (untreated) composite. However, at higher peroxide concentrations the mechanical properties followed a detrimental trend, indicating a more extensive attack on the poly(propylene) chains which can ultimately lead to degradation of the material. In addition, changes in crystallinity were proved to be dependent on the treatment condition, with higher concentrations of peroxide resulting in an overall lower degree of crystallization. Tensile modulus was found not to be directly related to the crystalline fraction, indicating the coexistence of several effects both in the composite's interface and the polymer microstructure.

Acknowledgements: The development of this work was partly financed by *Centro de Sistemas de Manufactura (CSIM)* through the *Centro de Planeación y Desarrollo of ITESM, Campus Monterrey*. One of the authors, LFRdeV, wishes to thank *CONACYT of Mexico* for partly financing this study through project SEP-2003-CO2-43983. Additionally, special thanks are due to the *Polymer Composites Group* at the *TUHH* in Germany for their valuable contributions to this thesis project.

Received: June 27, 2007; Revised: August 7, 2007; Accepted: August 17, 2007; DOI: 10.1002/mame.200700201

Keywords: carbon nanofibers (CNF); CNF functionalization; mechanical properties; poly(propylene); surface treatment

[1] Y. Lu, P. K. Liaw, *JOM* **2001**, *53*, 31.
[2] M. Meyyppan, D. Srivastava, "Carbon Nanotubes", in: *Handbook of nanoscience, engineering, and technology*, 3rd Edition, W. A. III, D. W. Goddard Brenner, S. E. Lyshevski, G. J. Lafrate, Eds., CRC Press, Boca Raton 2003, p. XVIII/1.
[3] R. H. Baughman, A. Zakhidov, W. de Heer, *Science* **2002**, *297*, 787.
[4] R. Baker, K. Terry, "Synthesis, properties and applications of graphite nanofibers", in: *R&D Status and trends in nanoparticles, nanostructured materials, and nanodevices in the United States*, World Technology Evaluation Center (WTEC), Baltimore, Maryland, USA 1997.
[5] K. Teo, C. Singh, M. Chhowalla, W. I. Milne, "Catalytic synthesis of carbon nanotubes and nanofibers", in: *Encyclopedia of nanoscience and nanotechnology*, Volume 1, H. S. Nalwa,

Editor in chief, American Scientific Publishers, California 2004, p. 665.
[6] E. V. Barrera, *JOM* **2000**, *52*, 38.
[7] B. S. Files, "Processing of carbon nanotubes for revolutionary space applications", in: *AIAA report*, American Institute of Aeronautics and Astronautics, 2000, p. 2000–5345.
[8] M. F. Yu, B. S. Files, S. Arepalli, R. Ruoff, *Phys. Rev. Lett.* **2000**, *84*, 5552.
[9] K. Lozano, E. V. Barrera, *J. Appl. Polym. Sci.* **2000**, *79*, 125.
[10] H. Ma, J. Zeng, M. L. Realff, S. Kumar, D. A. Schiraldi, *Compos. Sci. Technol.* **2003**, *63*, 1617.
[11] Available from: Applied Science Inc. http://www.apsci.com.
[12] J. Sandler, M. Shaffer, Y. M. Lam, A. H. Windle, P. Werner, V. Altstädt, J. Nastalczyk, G. Broza, K. Schulte, C. A. Keun, "*Carbon nanofiber-filled thermoplastic composites*", MRS 2001 Fall Meeting, Boston, MA, USA 2001.
[13] Y. Gao, P. He, J. Lian, L. M. Wang, D. Quian, J. Zhao, W. Wang, M. J. Schulz, J. Zhang, X. P. Zhou, D. L. Shi, *J. Macromol. Sci., Phys.* **2006**, *45*, 671.
[14] A. Kelarakis, K. Yoon, I. Sics, R. H. Somani, X. M. Chen, B. S. Hsiao, B. Chu, *Polymer* **2005**, *46*, 1159.
[15] A. Kelarakis, K. Yoon, I. Sics, R. H. Somani, X. M. Chen, B. S. Hsiao, B. J. Chu, *Macromol. Sci., Phys.* **2006**, *45*, 247.
[16] K. Wiemann, W. Kaminsky, F. H. Gojny, K. Schulte, *Macromol. Chem. Phys.* **2005**, *206*, 1472.
[17] K. Enomoto, T. Yasuhara, N. Ohtake, *New Diamond Frontier Carbon Technol.* **2005**, *15*, 59.
[18] B. A. Higgins, W. J. Brittain, *Eur. Polym. J.* **2005**, *41*, 889.
[19] E. Hammel, X. Tang, M. Trampert, T. Schmitt, K. Mauthner, A. Eder, P. Potschke, *Carbon* **2004**, *42*, 1153.
[20] I. C. Finegan, G. G. Tibbetts, D. G. Glasgow, J. M. Ting, M. L. Lake, *J. Mater. Sci.* **2003**, *38*, 3485.
[21] J. Sandler, G. Broza, M. Nolte, K. Schulte, Y. M. Lam, M. S. Shaffer, *J. Macromol. Sci., Phys.* **2003**, *42*, 479.
[22] K. Lozano, S. Yang, R. E. Jones, *Carbon* **2004**, *42*, 2329.
[23] P. Cortés, K. Lozano, E. V. Barrera, R. J. Bonilla, *J. Appl. Polym. Sci.* **2003**, *89*, 2527.
[24] W. Brandl, G. Marginean, V. Chirila, W. Warschewski, *Carbon* **2004**, *42*, 5.
[25] A. Bismarck, M. Pfaffernoschke, J. Springer, E. Schulz, *J. Thermopl. Compos. Mat.* **2005**, *18*, 307.
[26] Y. K. Choi, K. Sugimoto, S. M. Song, Y. Gotoh, Y. Ohkoshi, M. Endo, *Carbon* **2005**, *43*, 2199.
[27] R. D. Patton, C. U. Pittman, L. Wang, J. R. Hill, *Composites: Part A* **1999**, *30*, 1081.
[28] L. Valentini, J. Biagiotti, M. A. Lopez-Manchdo, S. Santucci, J. M. Kenny, *Polym. Eng. Sci.* **2004**, *44*, 303.
[29] W. Brockmann, "Adhesive bonding of polypropylene", in: *Polypropylene: An A-Z Reference*, 1st Edition, J. Karger- Kocsis, Ed., Kluwer Publishers, Dordrecht 1999, p. I/6.
[30] M. S. Dresselhaus, T. C. Chieu, M. Endo, *Phys. Rev. B* **1982**, *26*, 5867.
[31] G. W. Ehrenstein, G. Riedel, P. Trawiel, "*Praxis der Thermischen Analyse von Kunststoffen*", 1st Edition, Hanser, Munich 1998, p. 56.

Macromolecular Journals
DOI: 10.1002/mame.200700201